CONF-950740--15

IN-TANK FLUID SLOSHING EFFECTS DURING EARTHQUAKES: A PRELIMINARY COMPUTATIONAL SIMULATION

James E. Park
Mohamad A. Rezvani
Computing Applications Division
Oak Ridge National Laboratory*
Oak Ridge, Tennessee 37831

To be presented at
1995 ASME/JSME Pressure Vessels and Piping Conference
Honolulu, Hawaii
July 23-27, 1995

*Managed by Martin Marietta Energy Systems, Inc., for the U.S. Department of Energy under contract DE-AC05-84OR21400.

DISCLAIMER

Portions of this document may be illegible in electronic image products. Images are produced from the best available original document.

IN-TANK FLUID SLOSHING EFFECTS DURING EARTHQUAKES: A PRELIMINARY COMPUTATIONAL SIMULATION

James E. Park, mem. ASME[1]
Mohamad A. Rezvani[2]

ABSTRACT
Hundreds of underground radioactive waste storage tanks are located at Department of Energy (DOE) sites. At present, no technique for evaluating the pressure loads due to the impact of earthquake-generated waves on the side walls and dome of the tanks is known if the wave breaks back on itself. This paper presents the results of two-dimensional Computational Fluid Dynamics (CFD) calculations of the motion of waves in a generic rectangular tank as the result of accelerations recorded during an earthquake. The advantages and limitations of this technique and methods for avoiding the limitations will be discussed.

INTRODUCTION
Threat of Damage to Storage Tanks from Earthquake Loads - During World War II and the years immediately following, large volumes of toxic, explosive, and/or radioactive wastes were generated by the production of fissile material for the U. S. Atomic Energy Commission. Much of that waste is stored as liquids in large tanks at various government facilities. As these tanks age, a variety of safety-related concerns have emerged. Valenti (1993) has described some of the current problems at one DOE site.

One of the current challenges is to ensure the integrity of the storage tanks during an earthquake. Some of these tanks are filled to their design capacity of 3.8×10^6 L (1×10^6 gal.). During an earthquake, the surface waves generated by sloshing effects could apply excessive pressure on the free-board cylindrical part of the tank, the tank dome, and the knuckle (junction of the two) of the tank. Knowledge of the pressure distribution is an essential element in investigating the integrity of the tanks and resolving the related safety issues.

However, the response of the liquid in those tanks to the shaking of an earthquake is not well understood, that is, the responsible engineers do not have a technique for calculating the pressure generated by a wave breaking on the freeboard, knuckle, or dome of a storage tank. The safety of these aging repositories cannot be certified unless the motion of the stored liquid and its interaction with its container to earthquake loading can be forecast.

---

[1]Senior Development Staff, Oak Ridge National Laboratory (ORNL), TN

[2]Development Staff, Oak Ridge National Laboratory, Oak Ridge, TN

Computational Fluid Dynamic (CFD) Simulation of Wave Breaking - CFD was developed at the Los Alamos National Laboratory (LANL) in order to study the behavior of solids at very high pressures. A major off-shoot of that work was a series of algorithms specifically developed to simulate the motion of one or more fluids in which a void or liquid surface is present.

The first of these was the MAC (Marker-And-Cell) algorithm (Harlow and Welsh, 1965; and Welch et al., 1966), followed quickly by the SMAC (Simplified MAC) technique (Amsden and Harlow, 1970a, 1970b). Among the early successes for these methods were the first simulation of waves breaking on a beach and the splashing of a drop of liquid into a pool.

The MAC/SMAC algorithm was followed by the SOLA series of codes. In particular, an innovative approach to the simulation of free surface motion was embodied in the SOLA-VOF algorithm (SOLution Algorithm-Volume Of Fluid, Hirt and Nichols, 1981; and Nichols, Hirt, and Hotchkiss, 1980). The algorithm allows interfaces between a fluid and a void (a free surface) or between two fluids to be modeled in an especially sharp fashion. The concept was developed and refined in two codes developed to simulate the sloshing of liquids (oxidizer or fuel) in partially filled tanks in low or negligible gravity by Torrey and coworkers (Torrey et al., 1985, 1987). A recent advancement for free surface flows is presented by Kothe et al. (1991).

Alternatives to the VOF technique have been developed as well. A recent paper (Welsh, Trapp, and Mortensen, 1993) introduces an innovative counting technique to replace some of the more computationally intense portions of the VOF algorithm. Two recent papers by a team at Southern Methodist University (Raad, Chen, and Johnson, 1994; and Chen, Johnson, and Raad, 1994) introduce new algorithms to determine the fluid pressure near a free surface and to set velocity boundary conditions at a free surface. Also, Chen, Kelecy, and Pletcher (1994) map the free surface to one boundary of their coordinate system.

From this sampling of the history of CFD, it is clear that the complex interactive motion of free liquid surfaces can be predicted using CFD techniques. These techniques enable the analyst to numerically model the tank and the contents, simulate the fluid motion, and provide the fluid velocity at the surface as well as the pressure on the tank structure as a function of time. The pressure can then be used to evaluate the structural integrity of the tank.

DESCRIPTION OF TANK AND SAFETY CONCERN

A "reference tank" has been defined by the Westinghouse Hanford Company (Shrivastava and Weiner, 1993). The tank is cylindrical, with a vertical cylindrical axis (Fig. 1). The tank has a radius of 11.43 m (37.5 ft). The depth of liquid in the tank is 11 m (36 ft), yielding a capacity of 4.4×10^6 L (1.16 million gallons) of liquid waste. Above the freeboard, the tank is closed by a domed lid. The center of the dome is 14.9 m (49 ft) above the floor of the tank. The floor of the tank has a 3% slope from the wall to the center.

During an earthquake, two horizontal and a vertical acceleration are applied to the tank and the fluid. A typical acceleration history (Weiner, 1992) is shown in Fig. 2. The high-frequency oscillatory character of the accelerations is clear. It is expected that application of these accelerations to a tank partially filled with liquid will result in a sloshing motion of the fluid. If the freeboard is inadequate, the sloshing liquid will impact on the lid of the tank.

The objective of the CFD calculation is to apply the accelerations within the equation of motion for the fluid, to track the motion of the fluid, including the shape of the free surface(s) during the sloshing, and to calculate the evolution of the fluid pressure on the walls and the lid during the quake.

For this study, the tank structure is assumed to be rigid. It is shown (Velestos and Shivakumar, 1991; BNL, 1993) that sloshing effects are unaffected by the flexibility of the tank wall; the frequency of the fluid sloshing is much lower than the natural frequencies of the tanks of interest. Therefore, neglecting the elasticity of the tank walls when applying boundary conditions for the fluid motion has a negligible effect on the value of the calculated pressures generated by the moving fluid.

OUTLINE OF CFD PROCEDURE USED

The calculations presented in this paper were performed using the CFD code SOLA-VOF (Nichols, Hirt, and Hotchkiss, 1980). The code was developed at the Los Alamos National Laboratory and is available from the Energy Science and Technology Software Center.[3] The present version has been extensively modified at ORNL. However, the computational capability of the original version has not been compromised.

SOLA-VOF generates numerical solutions for the transient motion of an incompressible, viscous fluid in time and two spatial dimensions,

$$u_{,x} + w_{,z} = 0$$

$$u_{,t} = - uu_{,x} - wu_{,z} - p_{,x}/\rho + g_x + \nu(u_{,x,x} + u_{,z,z})$$

$$w_{,t} = - uw_{,x} - ww_{,z} - p_{,z}/\rho + g_z + \nu(w_{,x,x} + w_{,z,z})$$

where x and z are the horizontal and vertical coordinates; u and w are the horizontal and vertical components of the fluid velocity, p is the pressure, ρ is the fluid density, ν is the kinematic viscosity, and g_x and g_z are components of the body acceleration. These equations are statements of mass conservation and Newton's second law of motion, in which, for example,

$$u_{,t} = \frac{\partial u}{\partial t} .$$

---

[3]P.O. Box 1020, Oak Ridge, TN 37831, (615) 576-2606 - Pkg # 274-C7600-00.

The solution is obtained by finite-difference techniques on a regular (rows and columns) mesh. Irregular shapes may be approximated by collections of rectangular obstacles, that is, a curved boundary is approximated by stair-stepping. The transient motion of interest is simulated as a series of short steps in time, or computational cycles. Starting with the initial conditions for the problem – a mathematical description of the shape, velocity and pressure of the fluid – each cycle is divided into three phases.

First, tentative new values for the velocity (horizontal and vertical components) are calculated by applying pressure and viscous forces, by advecting fluid from neighboring regions of the fluid, and by applying the accelerations due to the earthquake being simulated. Second, mass continuity is enforced by solving a Poisson equation for the pressure change at each point in the fluid and updating the tentative velocities in response to the change in pressure. Finally, the Volume of Fluid (VOF) algorithm is applied to move the fluid at its surface, allowing propagation of any free surfaces and interaction with any solid boundaries included in the problem. Boundary conditions are imposed on the fluid at appropriate points within the time step.

At the end of each cycle, the time step is adjusted in response to the changes in velocity and surface location. The maximum time step that can be used for numerical stability is the smaller of the minimum time required for information to convect or diffuse across any cell on the computational mesh. In addition, the allowable time step may be limited by the surface tension or the speed of surface waves. Details are given in Hirt and Nichols (1981).

For this work, the allowable time step was further limited to ensure that several computational cycles were taken between each acceleration data point. The acceleration data for the earthquake to be simulated are stored in tabular form, $g_{ex}(t)$, $g_{ey}(t)$, *and* $g_{ez}(t)$. If Δt is the time between data points and δt_s is the time step allowed by the stability criteria, the following adjustment was made. First, the number of increments required by the stability criteria was calculated.

$$N_{stab} = \text{integer}\{\Delta t/\delta t_s + 1\}.$$

This value was compared with the number of cycles per data point selected to establish sufficient resolution,

$$N_{appl} = \max\{N_{stab}, N_{res}\}.$$

Finally, the applied time step was calculated,

$$\delta t_s = \Delta t/N_{appl}.$$

The stability criteria were checked at the end of each computational cycle, and δt_s was adjusted as needed. After the time step was selected, the computational time was advanced, $t^{n+1} = t^n + \delta t_s$, and the measured acceleration data were interpolated to give the value applied to the fluid at the computational time t^{n+1}. For each time step during the integration, the horizontal acceleration is applied to the horizontal component of the equations of motion,

$$g_x = g_{ex}(t^{n+1}),$$

and the vertical acceleration due to the earthquake is added to the gravitational acceleration,

$$g_z = g_{grav} + g_{ez}(t^{n+1}).$$

DESCRIPTION OF MODEL PROBLEM

Computational Model - Because the SOLA-VOF code is two-dimensional (2-D), the cylindrical tank (Fig. 1) has been represented by a 2-D slice through the tank. The resulting rectangle is 20 m wide, and the distance from the floor of the tank to the roof is 11.3 m. The slope of the floor is not modeled. Using SOLA-VOF, the domed roof could be represented by stair-stepping or simply replaced by a flat roof. We have chosen to use a flat roof.

The rectangular tank was initially filled with fluid to a depth of 11 m, leaving a freeboard of 0.3 m (1 ft). The density of the fluid is 1,500 kg/m^3.

Initial Conditions - At the beginning of the simulation, before the earthquake starts, the fluid is at rest in the tank, that is, the velocities are zero. The pressure is hydrostatic; the vertical pressure gradient is balanced by gravity. The pressure above the fluid is assumed to be negligible.

Boundary Conditions - The walls and lid are rigid. At the walls of the tank, no fluid is allowed to leave the tank and viscous shear is neglected, that is, the normal velocity is zero and the gradient of the tangential velocity is zero. At liquid surfaces, the normal stress is equal to the applied pressure (negligible for these calculations).

Finite-Difference Mesh - The rectangular problem region was divided into 76 equal-width (0.263-m) cells horizontally by 35 zones vertically. Eighteen equal-height zones were used between the elevations of 8.8 and 11.3 m, yielding a cell height of 0.15 m in the region in which the fluid motion was most violent. That computational mesh is shown on Fig. 3. For about the first 9 s of the simulation, a refined mesh was used for a separate calculation. The horizontal resolution was not changed, but the number of zones in the upper portion of the tank was increased from 18 to 25, reducing the constant cell height from 0.15 cm to 0.10 cm.

PRESENTATION AND DISCUSSION OF RESULTS

The results are shown as plots of the surface shape at various times during the simulation. In SOLA-VOF, the surface is identified with computational cells in which the fraction occupied by fluid is

$$\epsilon < f < 1.0 - \epsilon,$$

where f is the volume fraction of fluid in a particular computational cell and ϵ is usually taken to be about 1×10^{-6}. If $f > 1.0 - \epsilon$, then f is set to 1 (the cell is treated as being *full* of fluid). If $f < \epsilon$, f is set to 0 and the cell is treated as *empty*. The contours shown on the following figures are for the value $f = 0.1$.

Figures 4 and 5 show the surface shape at times of 4.0 and 8.0 s. Clearly the two solutions are similar, and, as indicated by the difference between the two curves, both meshes are too coarse. Further, experimentation with the contour value of f used to represent the liquid surface shows that the structure of the surface depends on the value chosen. For example, the contour $f = 0.0$ would show more local "bumps" than the contour $f = 0.1$ shown in the figures. This ambiguity in the location of the liquid surface can be reduced by using a refined computational grid. One possible method has been developed by Raad, Chen, and Johnson, 1994.

In Fig. 5, the liquid crest is about 0.5 m above the lowest level. In Fig. 6, the wave is in intimate contact with the lid of the tank. In Fig. 7 (10 s and 16 s), a secondary surge with a great deal of structure is starting to develop. The final frame (Fig. 8), at 17.1 s, shows four smaller surges. Shortly after this time was reached, the pressure equation algorithm failed. Using a third mesh, the algorithm failed at about 20 s.

The pressure equation algorithm in SOLA-VOF must be supplemented by a more modern algorithm. One alternative, the conjugate residual technique, has been implemented by Torrey et al. (1985, 1987). Another possibility is successive over-relaxation by lines (Park and Cross, 1980).

CONCLUSION AND ADDITIONAL WORK REQUIRED

CFD can be used to calculate the sloshing motion of a partially confined liquid, including the shape of the liquid surface, due to earthquake motion of the tank containing the liquid.

This study has identified several problems that must be resolved before SOLA-VOF can be used by tank design and earthquake damage forecasting professionals:

1. Demonstration calculations must be extended to three-dimensional geometries.
2. CFD predictions must be compared with existing test data.
3. Curved tank walls, such as the knuckle and dome regions of the reference tank, must be included in any credible model (Sicilian and Hirt, 1984, show a method for doing this using a finite difference code such as SOLA-VOF).
4. The solid crust that sometimes forms on the surface of the liquid (Valenti, 1993) will have a strong influence on the motion of the liquid during an earthquake. At this time, it is not clear how this should be handled.
5. Further CFD simulations of sloshing due to earthquake motion will require use of a more modern algorithm to handle pressure calculation and velocity boundary conditions at the free surface.
6. A more robust solution algorithm must be used for the pressure/continuity equation.
7. The region of the fluid in which the sloshing occurs will require better resolution (more computational cells) than that used for the present work.

Commercial CFD codes may have addressed many of these problems.

REFERENCES

Amsden, A. A. and Harlow, F. H., 1970a, *The SMAC Method: A Numerical Technique for Calculating Incompressible Fluid Flows*, LA 4370, Los Alamos Scientific Laboratory, Los Alamos, NM.

Amsden, A. A. and Harlow, F. H., 1970b, "A Simplified MAC Technique for Incompressible Fluid Flow Calculations," *J. Comp. Physics*, Vol. 6, pp. 322-325.

BNL, 1993, *U.S. Department of Energy, Seismic Design and Evaluation Guidelines for the Department of Energy High-Level Waste Storage Tanks and Appurtenances*, BNL-52361, Brookhaven National Laboratory, Associated Universities, Inc., Upton, NY.

Chen, Huo-Huey, Kelecy, Franklyn J., and Pletcher, Richard H., 1994, "Numerical and Experimental Study of Three-Dimensional Liquid Sloshing Flows," *J. Thermophysics and Heat Transfer*, Vol. 8, No. 3, pp. 507-513.

Chen, Shea, Johnson, David B., and Raad, Peter B., 1994, "Velocity Boundary Conditions for the Simulation of Free Surface Fluid Flow," *Individual Papers in Fluids Engineering, 1994*, ASME FED-Vol. 202, pp. 55-66.

Harlow, F. H., Shannon, J. P., and Welch, J. E., 1965, "Liquid Waves of Computer," *Science*, Vol. 149, p. 1092.

Harlow, F. H. and Welch, J. E., 1965, "Numerical Calculation of Time-Dependent Viscous Incompressible Flow of fluid with Free Surface," *Phys. Fluids*, Vol. 8, pp. 2182-2189.

Hirt, C. W. and Nichols, B. D., 1981, "Volume of Fluid (VOF) Method for the Dynamics of Free Boundaries," *J. Comp. Physics*, Vol. 39, pp. 201-225.

Kothe, Douglas B., Mjolsness, Raymond C., and Torrefy, Martin D., 1991, *RIPPLE: A Computer Program for Incompressible Flows with Free Surfaces*, LA-12007-MS, Los Alamos National Laboratory, Los Alamos, NM.

Nichols, B. D., Hirt, C. W., and Hotchkiss, R. S., 1980, *SOLA-VOF: A Solution Algorithm for Transient Fluid Flow with Multiple Free Boundaries*, LA 8355, Los Alamos Scientific Laboratory, Los Alamos, NM.

Park, James E. and Cross, Kenneth E., 1980, *Calculation of Fluid Circulation Patterns in the Vicinity of Submerged Jets Using ORSMAC*, K/CSD-4, Union Carbide Corporation - Nuclear Division, Oak Ridge, TN.

Raad, Peter B., Chen, Shea, and Johnson, David B., 1994, "The Introduction of Micro Cells to Treat Pressure in Free Surface Fluid Flow Problems," *Individual Papers in Fluids Engineering, 1994*, ASME FED-Vol. 202, pp. 43-54.

Shrivastava, H. P., and Weiner, E. O., 1993, "Structural Design Requirements and Guidelines for the Multi-Functional Waste Tanks," *Proceedings, Fourth DOE Natural Phenomena Hazards Mitigation Conference*, Atlanta, GA, pp. 619-625.

Sicilian, J. M., and Hirt, C. W., 1984, "An Efficient Computation Scheme for Tracking Contaminant Concentrations in Fluid Flows," *J. Comp. Phys*, Vol. 56, p. 428.

Torrey, Martin D., Cloutman, Lawrence D., Mjolsness, Raymond C., and Hirt, C. W., 1985, *NASA-VOF2D: A Computer Program for Incompressible Flow with Free Surfaces*, LA-10612-MS, Los Alamos National Laboratory, Los Alamos, NM.

Torrey, Martin D., Mjolsness, Raymond C., Stein, Leland R., 1987, *NASA-VOF3D: A Computer Program for Incompressible Flow with Free Surfaces*, LA-11009-MS, Los Alamos National Laboratory, Los Alamos, NM.

Valenti, Michael, 1993, "Taming Hanford's most troublesome nuclear waste tank," *Mech. Eng.*, Vol. 115, No. 11, pp. 68-72.

Velestos, A. S., and P. Shivakumar, 1991, "Hydrodynamic Effect in Tanks with Different Conditions of Support," *Proceedings, Third DOE Natural Phenomena Hazards Mitigation Conference*, St. Louis, MO, October, 1991, pp. 578-587.

Weiner, E. O., 1992, *Design Basis Earthquake Time Histories for 1992 SDC-4.1, Revision*, WHC-SD-GN-30018, (September), Westinghouse Hanford Company, Richland, WA.

Welch, J. E., Harlow, F. H., Shannon, J. P., and Daly, B. J., 1966, *THE MAC METHOD, A Computing Technique for Solving Viscous, Incompressible, Transient Fluid-Flow Problems Involving Free Surfaces*, LA 3425, Los Alamos Scientific Laboratory, Los Alamos, NM.

Welch, Sam, Trapp, John, and Mortensen, Glen, 1993, "Interface Tracking in Two-Phase Flow Simulations Using a Simple Subgrid Counting Procedure," *ASME paper presented at the Fluids Engineering Meeting*.

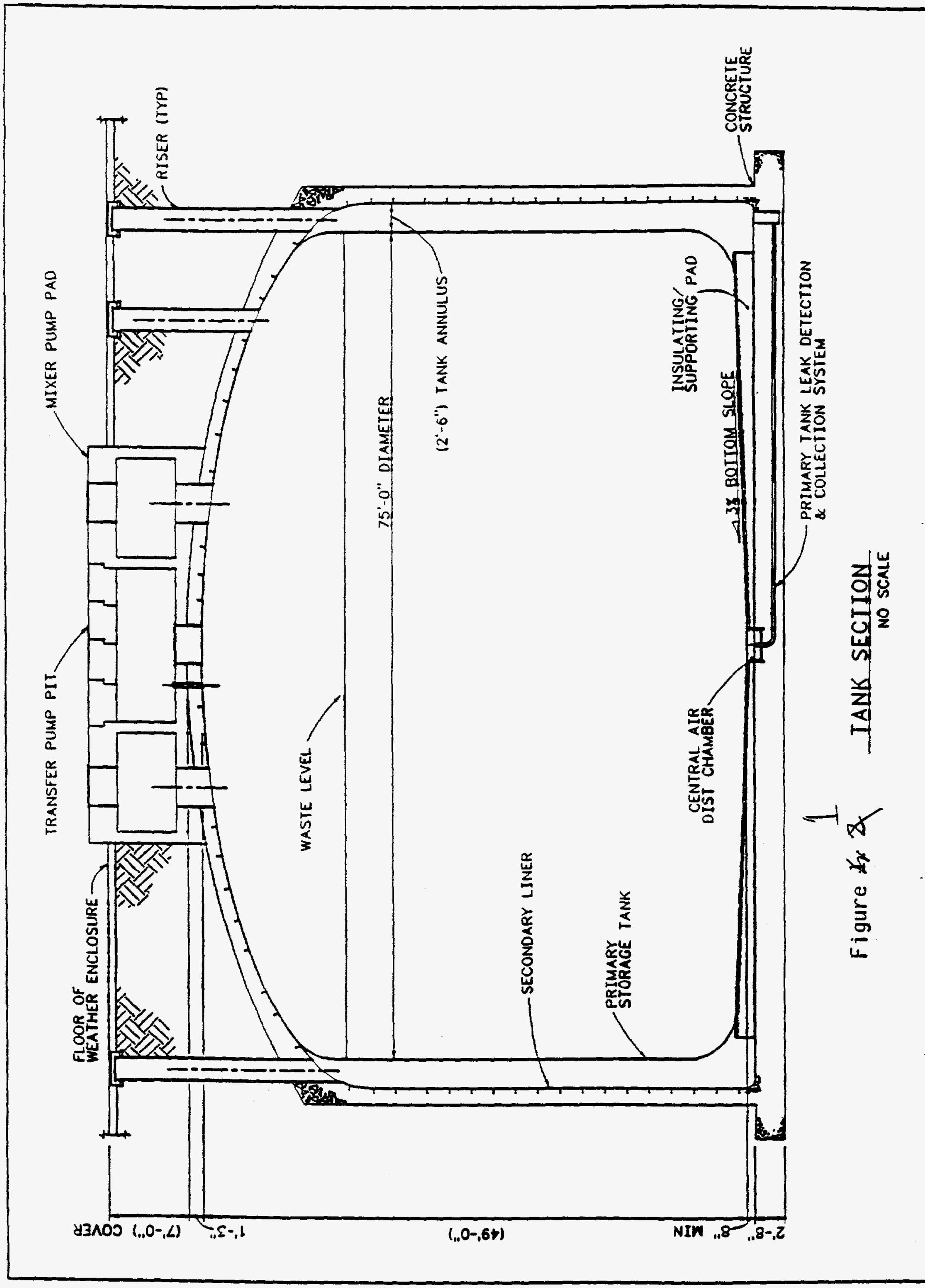

Figure 1

TANK SECTION
NO SCALE

fig 2

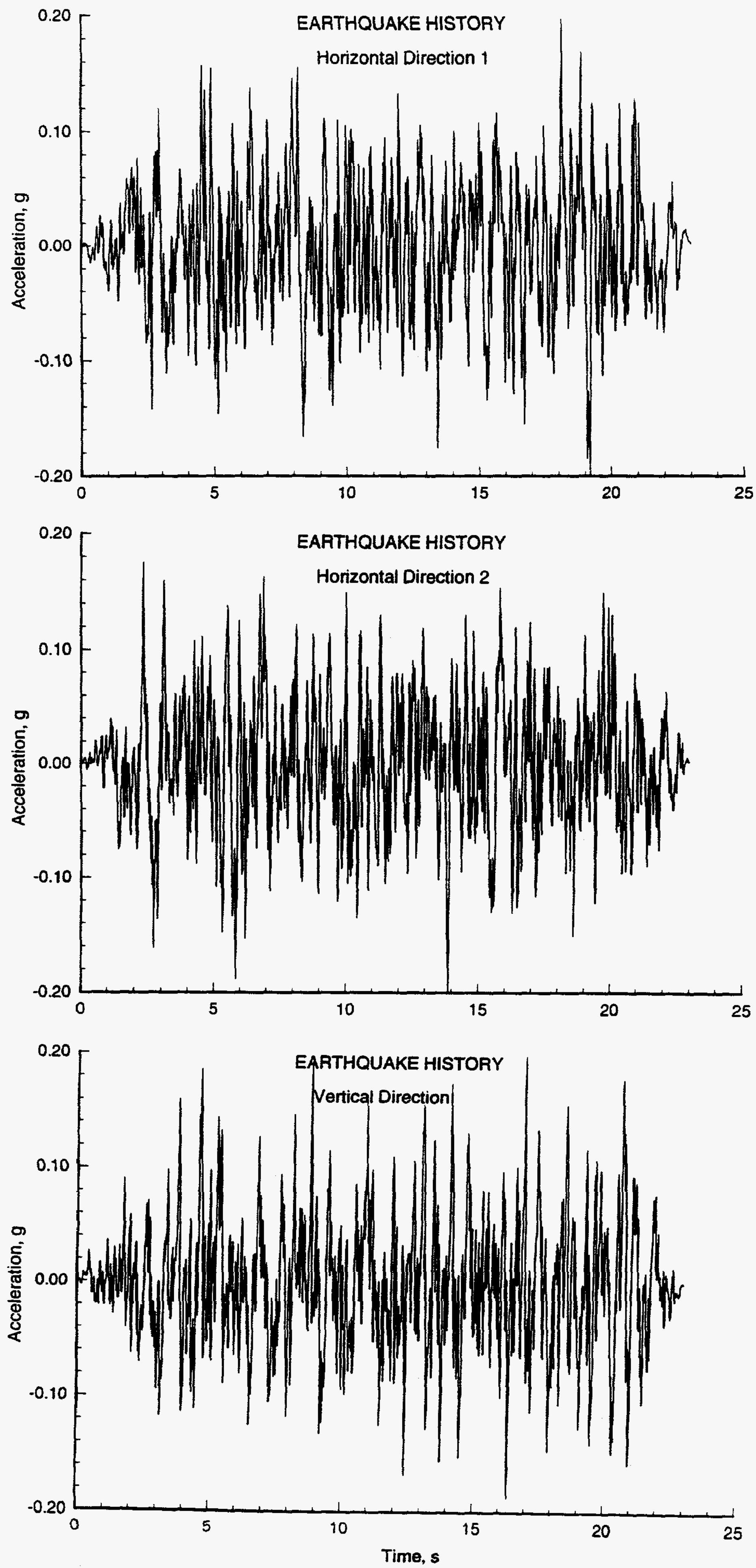
EARTHQUAKE HISTORY
Horizontal Direction 1
Acceleration, g
0.20
0.10
0.00
-0.10
-0.20
0
5
10
15
20
25
EARTHQUAKE HISTORY
Horizontal Direction 2
Acceleration, g
0.20
0.10
0.00
-0.10
-0.20
0
5
10
15
20
25
EARTHQUAKE HISTORY
Vertical Direction
Acceleration, g
0.20
0.10
0.00
-0.10
-0.20
0
5
10
15
20
25
Time, s

(2D) II Print II 25 Oct 1994 II tecfile.plt II

fig 3

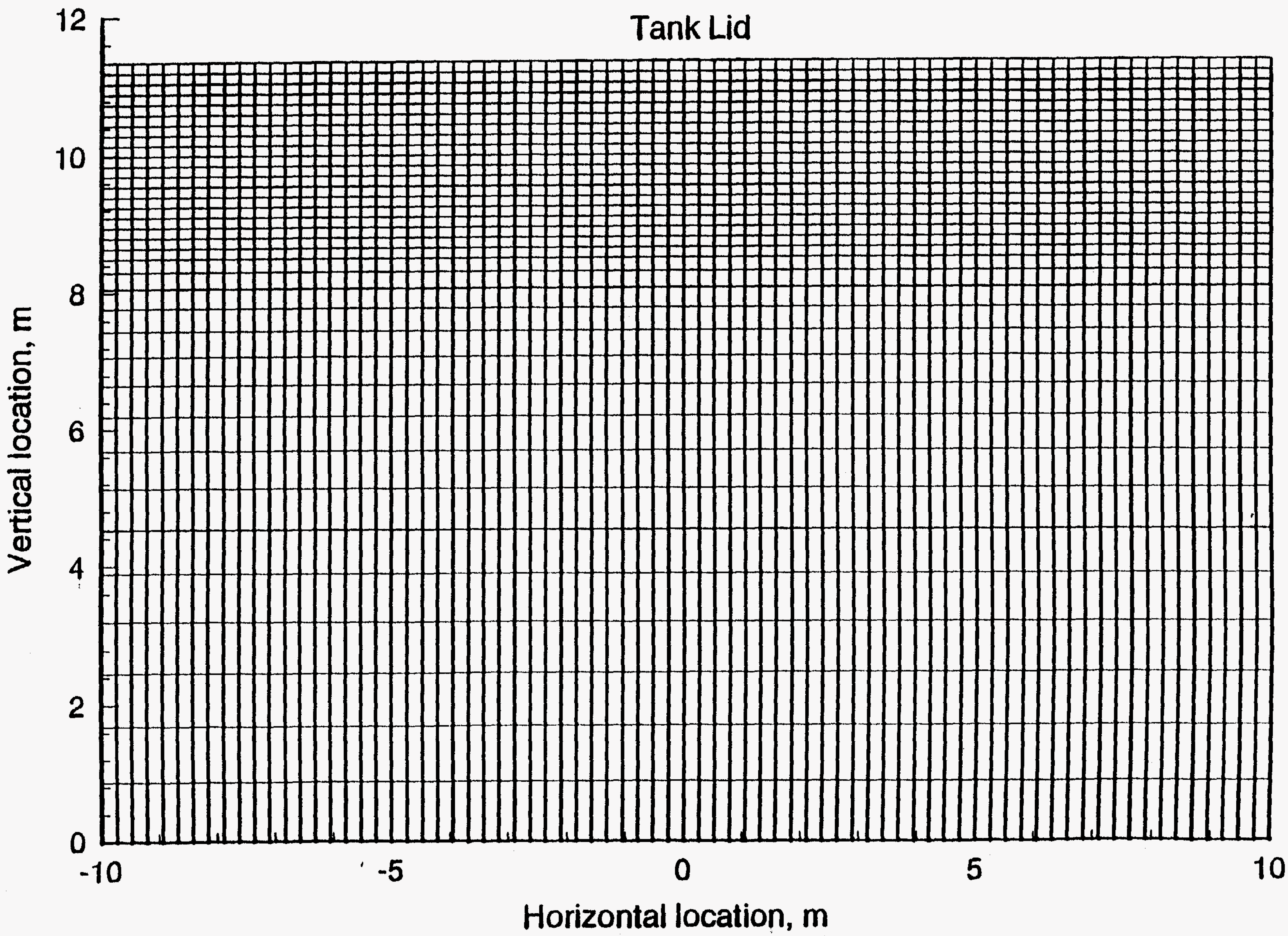

fig 4

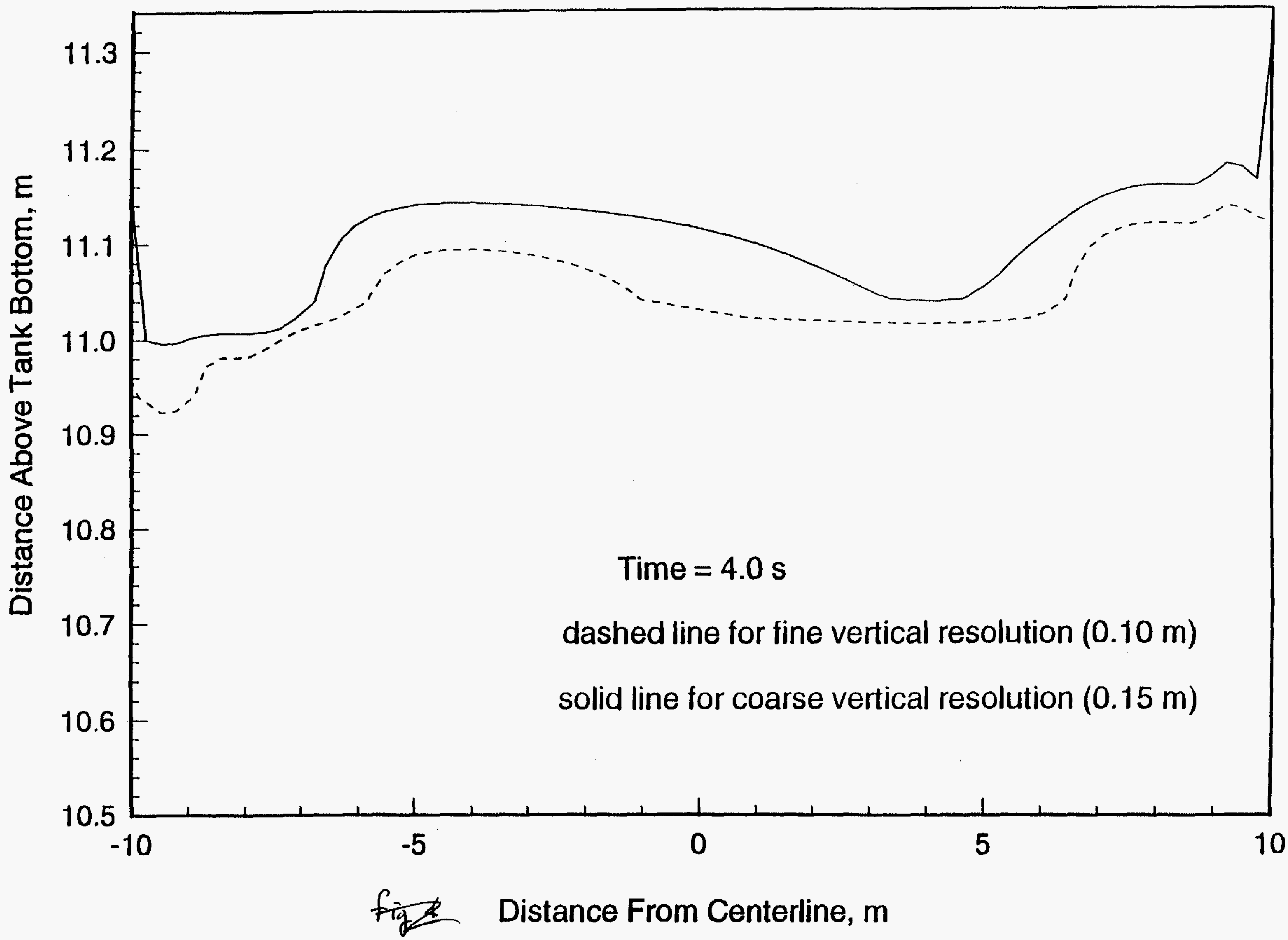

11.3
11.2
11.1
11.0
10.9
10.8
10.7
10.6
10.5
Distance Above Tank Bottom, m
-10
-5
0
5
10
Time = 4.0 s
dashed line for fine vertical resolution (0.10 m)
solid line for coarse vertical resolution (0.15 m)
Distance From Centerline, m

fig 5

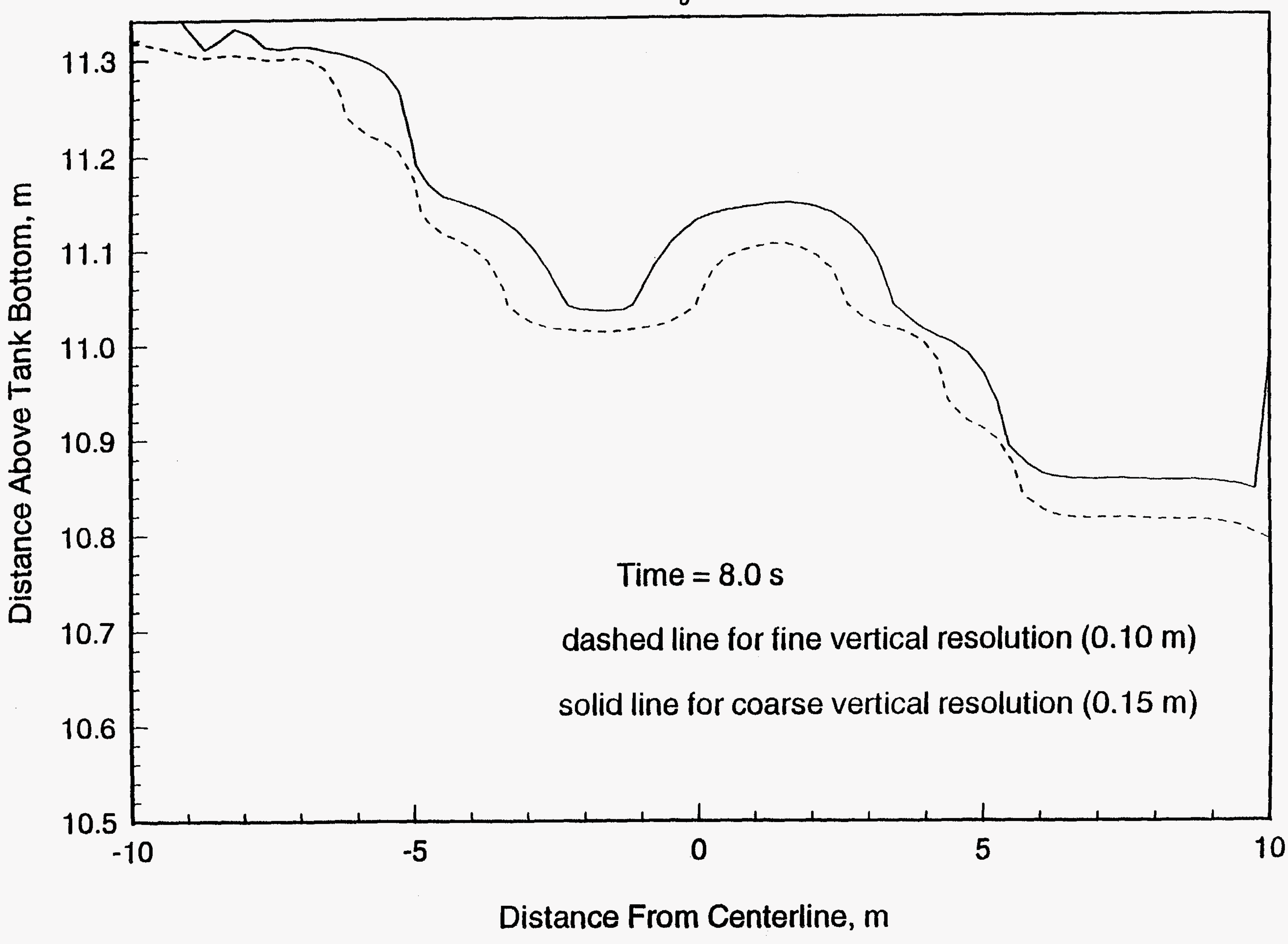

Distance Above Tank Bottom, m
11.3
11.2
11.1
11.0
10.9
10.8
10.7
10.6
10.5
-10
-5
0
5
10
Time = 8.0 s
dashed line for fine vertical resolution (0.10 m)
solid line for coarse vertical resolution (0.15 m)
Distance From Centerline, m

fig 6

(2D) || Print || 14 Nov 1994 || finetop.plt ||

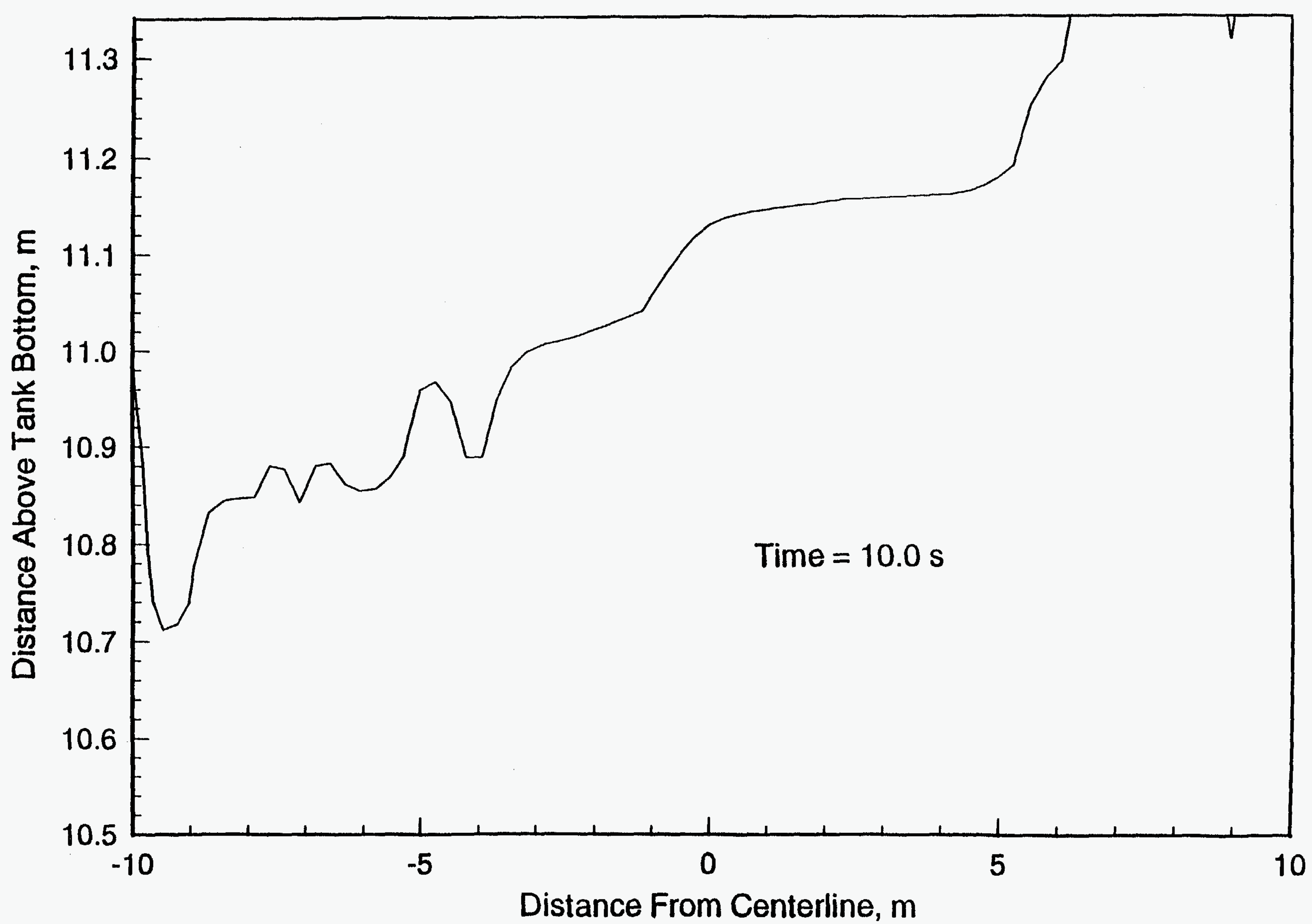

fig 7

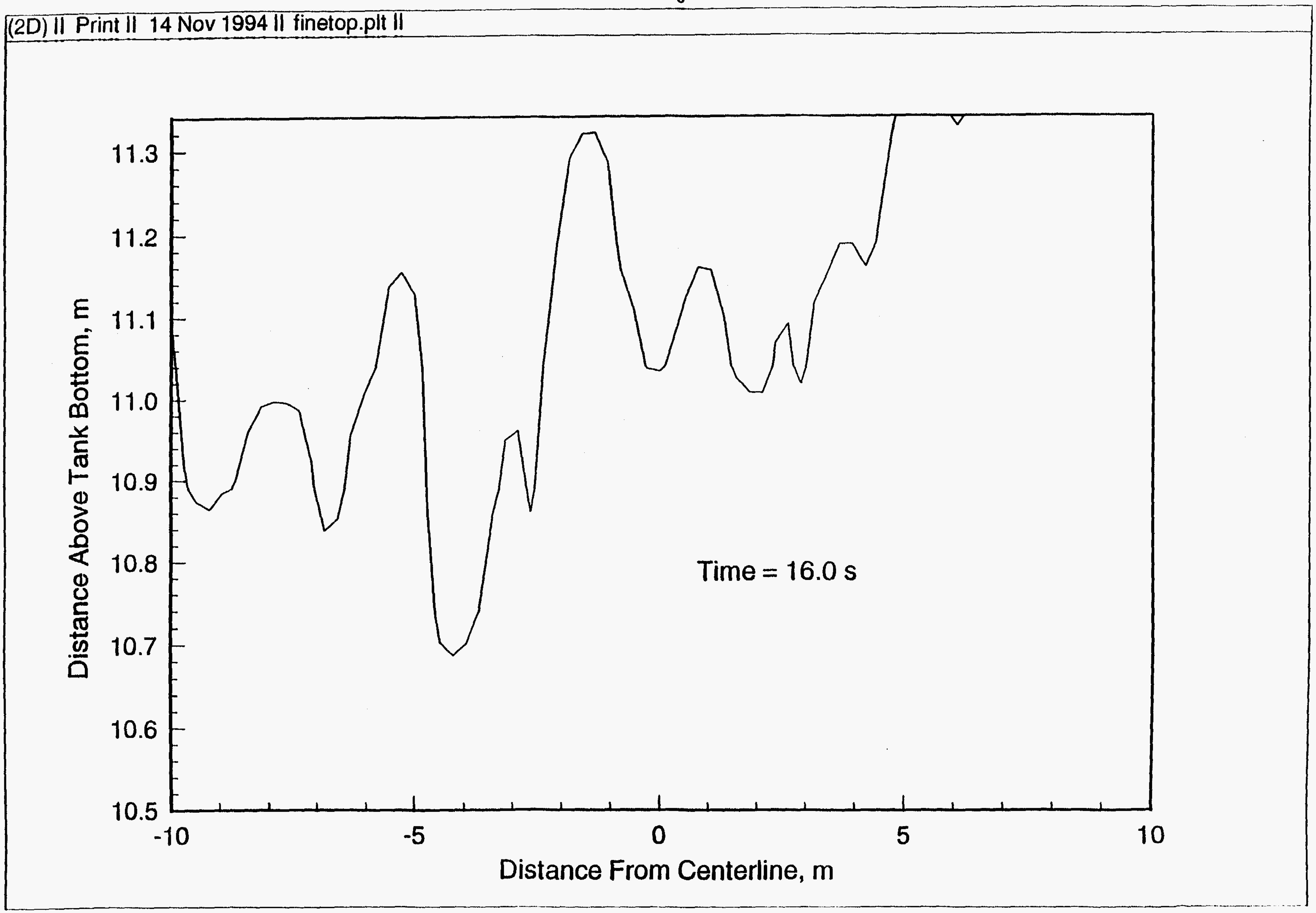

(2D) II Print II 14 Nov 1994 II finetop.plt II
Distance Above Tank Bottom, m
11.3
11.2
11.1
11.0
10.9
10.8
10.7
10.6
10.5
-10
-5
0
5
10
Distance From Centerline, m
Time = 16.0 s

fig 8

(2D) || Print || 14 Nov 1994 || finetop.plt ||